

Monolithic Trace-Contaminant Sorbents Fabricated from 3D-printed Polymer Precursors

Marek A. Wójtowicz[1], Joseph E. Cosgrove[2], and Michael A. Serio [3], Andrew E. Carlson[4]
Advanced Fuel Research, Inc., 87 Church Street, East Hartford, CT 06108-3720, USA

and

Cinda Chullen[5]
NASA Johnson Space Center, 2010 NASA Parkway, Houston, TX 77058

The current trace-contaminant (TC) removal technology for use in Extravehicular Activities (EVAs) involves the use of a packed bed of acid-impregnated granular charcoal, which is difficult to regenerate. In this paper, results are presented on the development of vacuum-regenerable TC sorbents for use in the Portable Life Support System (PLSS). The sorbents are derived from 3D-printed polymer monoliths (e.g., honeycomb structures), which are then carbonized and activated in order to develop porosity, and also to enhance the TC-sorption capacity. Results are presented on the following aspects of carbon-sorbent development: (1) precursor selection; (2) monolith fabrication; (3) shape retention and strength; (4) carbon surface and porosity characterization; (5) TC-sorption capacity and vacuum-regeneration; (6) pressure drop; and (7) sub-scale sorbent prototype. The use of predominantly microporous monolithic carbon is associated with the following benefits: (a) high TC-sorption capacity; (b) low pressure drop; (c) rapid vacuum (pressure-swing) desorption due to thin monolith walls and low pressure drop; (d) good thermal management (high thermal conductivity and low adsorption/desorption thermal effects associated with physisorption); and (e) good resistance to dusty environments.

Nomenclature

3D	=	three-dimensional
AFR	=	Advanced Fuel Research, Inc. (AFR)
CF	=	carbon fiber
D	=	monolith diameter
D_H	=	monolith hydraulic diameter
DFT	=	Density Functional Theory
d_p	=	pore size
EVA	=	Extravehicular Activity
f	=	friction factor
FTIR	=	Fourier Transform Infrared (spectroscopy, analysis, analyzer, etc.)
IUPAC	=	International Union of Pure and Applied Chemistry

1 Vice President, Clean Energy & Carbon Materials, Advanced Fuel Research, Inc., 87 Church Street, Suite 308, East Hartford, CT 06108
2 Senior Engineer, Advanced Fuel Research, Inc., 87 Church Street, Suite 308, East Hartford, CT 06108
3 President, Advanced Fuel Research, Inc., 87 Church Street, Suite 308, East Hartford, CT 06108
4 Senior Engineer, Advanced Fuel Research, Inc., 87 Church Street, Suite 308, East Hartford, CT 06108
5 Project Engineer, EVA Technology Development, NASA Johnson Space Center, 2101 NASA Parkway/EC5, Houston, TX 77058

L	=	monolith height
$LiOH$	=	lithium hydroxide
MFC	=	mass-flow controller
n	=	monolith cell density (cells per square inch)
PC	=	polycarbonate
$PEEK$	=	polyether ether ketone
PEI	=	polyetherimide
$PLSS$	=	Portable Life Support System
PVC	=	polyvinyl chloride
$PVDC$	=	polyvinylidene chloride
Re	=	Reynolds number
S_{BET}	=	BET (Brunauer, Emmett, and Teller) surface area (m^2/g)
TC	=	trace contaminant
TGA	=	thermogravimetric analyzer
u	=	gas velocity
$UTAS$	=	UTC Aerospace Systems
V_{micro}	=	micropore volume (cm^3/g)
V_p	=	(total) pore volume (cm^3/g)
XPS	=	X-Ray Photoelectron Spectroscopy
Δp	=	pressure drop
ΔV_2	=	pore volume in the range of pore widths 0.9–2.2 nm (cm^3/g)
δ_{ow}	=	monolith outer wall thickness
δ_w	=	monolith wall thickness
ε	=	monolith voidage
μ	=	gas dynamic viscosity
ρ	=	gas density
σ	=	monolith geometric surface area per unit volume (cm^2/cm^3)
*	=	Superscript * indicates values (of specific surface area, pore volume, etc.) expressed per gram of polymer-derived carbon, i.e. excluding the weight of the carbon fiber used as reinforcement.

I. Introduction

THE development of regenerable life support systems is critically important for the advancement of NASA's space-exploration projects. In addition to carbon dioxide (CO_2) and water vapor (H_2O) control, trace-contaminant (TC) removal plays a key role in life support systems, ensuring high quality air for the crew during Extravehicular Activities (EVAs) and also on board spacecraft. This paper addresses the fabrication of structured (monolithic), carbon-based TC sorbents for the space suit used in EVAs. The approach to sorbent fabrication involves the following steps: (1) preparation of the precursor material (polymer) in a desired shape using 3D printing; (2) precursor carbonization (pyrolysis) to produce a carbon monolith; and (3) monolith activation to obtain the desired pore-structure characteristics and TC-sorption performance (high sorption capacity and rapid vacuum-regeneration). The objectives of this study were: (1) to demonstrate the feasibility of using 3D printing to create plastic monoliths with complex geometries, e.g., honeycomb structures, subsequently converted into effective TC sorbents upon carbonization and activation, while preserving much of their original shape and strength; (2) to demonstrate effective ammonia and formaldehyde removal in the presence of CO_2 and humidity; also, rapid sorbent regeneration; and (3) to deliver a sub-scale sorbent prototype to NASA for further testing.

The starting materials for the sorbent-fabrication process are polymer-based precursors that produce microporous carbon upon carbonization (pore size $d_p < 2$ nm). (Such materials should be more correctly referred to as *nanoporous* carbon, even though the IUPAC recommends the term *microporous.*[1] The term *microporous* is used in this paper for the sake of consistency with IUPAC.) The use of the predominantly microporous monolithic carbon is associated with the following benefits: (a) high trace contaminant sorption capacity; (b) low pressure drop; (c) rapid vacuum (pressure-swing) desorption due to thin monolith walls and low pressure drop; (d) good thermal management (high thermal conductivity and low adsorption/desorption thermal effects associated with physisorption); and (e) good resistance to dusty environments. The expected fully regenerable sorbent-system operation that will result from this project is in contrast to the currently used EVA air-revitalization systems, which involve oversized, non-regenerable packed beds of activated carbon (AC) for TC control.

The currently available polymer-supported amine based CO_2-removal system developed at Hamilton Sundstrand, currently Collins Aerospace, offers a viable alternative to LiOH,[2,3] and is in fact used as a benchmark for future CO_2-removal systems. The amine-based sorbent (SA9T) is efficient and reliable, but it has the following drawbacks: (1) no, or only limited, trace-contaminant control;[4] (2) sorbent fouling caused by irreversible reactions with aldehydes;[5] and (3) complex behavior with respect to the possible ammonia offgassing[6] versus removal[7]. In addition, there is a concern about the possibility of a sudden release of large amounts of TCs, notably ammonia, which originate from equipment outgassing after a space suit has not been used for some time. In general, the trace contaminants of primary interest are ammonia and formaldehyde as they are the only ones that are likely to exceed the SMAC levels within the space suit.[8] Acetaldehyde is also of interest since it may degrade the operation of the CO_2-removal unit, but this study was concerned only with ammonia and formaldehyde removal.

Trace-contaminant removal in spacecraft environments has a long history, and it was reviewed by Paul and Jennings[9] of NASA Johnson Space Center. It was concluded that "there is currently no technology that is used in any industry that will perform better than activated charcoal for the PLSS application." Several approaches to carbon regeneration have been attempted (reverse airflow, steam regeneration, and vacuum regeneration), but the challenge of excessive regeneration temperature, and of long desorption time scales, remains to be resolved. In our prior work, we addressed this problem through tailoring the porous structure of carbon sorbents, and through the use of oxidative carbon-surface pretreatment.[10–13] In spite of the tremendous progress made (vacuum regeneration possible and the enhancement of sorption capacity as a result of surface oxidation), vacuum regeneration time at room temperature is still substantial (0.25–12 h). In addition, the manufacture of sorbent monoliths was crude (manually drilled holes), which resulted in large monolith channel wall thickness and significant gas-diffusion resistance. In addition, only polyvinylidene chloride (PVDC) was used in our previous work,[10–26] with carbon sorbents derived from other polymers still to be explored. The present study addresses the above challenges through the use of 3D printing and polymers that produce highly microporous carbons upon carbonization and activation. It should be noted that PVDC is not compatible with 3D printing, mainly due to the release of large amounts of hydrogen chloride upon heating.

The approach to TC sorption used in this work is based on physisorption on highly microporous carbon derived from polymers. The pore sizes are close to molecular dimensions, which ensures sufficiently strong van der Waals forces to obtain high TC-sorption capacities. In contrast, most commercial activated carbons contain only a small or modest percentage of microporosity, and this is why their sorption-capacity performance is low or modest, unless enhanced by chemisorption on acidic sites. The fact that the underlying principle for our sorbents is physisorption, rather than chemisorption makes vacuum and thermal regeneration fast and reversible. Also, the high purity of the carbon derived from polymer precursors makes it possible to keep the carbon surface acidity low, which facilitates the reversible TC sorption.

II. Materials and Experimental Procedures

A. Precursor Selection

Since testing all the possible polymer-filament formulations that are used in 3D printing was beyond the scope of this study, three polymers were initially chosen, and then one of them was down-selected for further work. The following criteria were used for precursor selection:

- compatible with 3D printing
- good shape retention upon carbonization and activation
  (A high carbon yield during carbonization, i.e. a low volatile-matter content, is favorable for shape retention; furthermore, high carbon yields improve process economics)
- good TC sorption and sorbent regeneration

To ensure that the polymers selected for the project were indeed compatible with 3D printing, it was decided that only commercially available 3D printing filaments would be used in the study. Three such polymer-based filaments were ordered and received from 3DXTECH, some of them reinforced with ~10 wt% carbon fiber (CF): polyether ether ketone (PEEK and PEEK/CF), polyetherimide (PEI/CF), also known as Ultem, and polycarbonate (PC and PC/CF). PEEK powder, supplied by Goodfellow USA, was also used in some experiments.

B. Carbonization and Activation

A standard laboratory tube furnace was used for carbonization, and several heating profiles were utilized, some of them with a single heating rate of 5 K/min, others with hold times at about 500 °C. The final carbonization

temperature used was 800 °C, and nitrogen was used as a carrier gas. In several experiments, polymer/carbon-fiber filament samples were rapidly inserted into the tube furnace preheated to 450 °C, 500 °C, 550 °C, and 600 °C, and held at the above temperatures for ~30 min. It was found that the carbonization conditions did not have a strong effect on shape retention for the PEEK polymer. For this reason, unless indicated otherwise, only results obtained using a heating rate of 5 K/min are reported. Carbon activation was carried out in a flow of air at 325 °C to a burn-off of ~18 wt% using a tube furnace.

C. Pore-Structure Characterization

An automated gas-sorption system Quantachrome ASiQwin was used for collecting and processing nitrogen-isotherm data for carbon sorbents. Prior to adsorption-isotherm measurements, each sample was outgassed under vacuum at 300 ºC for at least 3 hours. Nitrogen-adsorption isotherms were determined at 77 K, and these data were used to perform the following analyses: (a) Brunauer, Emmett, and Teller (BET) surface area; (b) pore volume; (c) Dubinin-Radushkevich (D-R) micropore surface area and micropore volume; and (d) pore-size distribution of micropores using the Density Functional Theory (DFT).

D. Sorbent Testing

The ammonia and formaldehyde sorption capacities were determined using the apparatus shown in Figure 1. The measurements of both cyclic and total (equilibrium) TC sorption capacity of sorbents were possible. The testing was performed in two stages: (a) NH_3/formaldehyde adsorption, where the gas stream was passed through the sorbent at pressures close to atmospheric; and (b) NH_3/formaldehyde desorption, where the sorbent was exposed to vacuum. The test cell containing the TC sorbent was placed in a temperature-controlled enclosure (not shown in Figure 1). $CO_2/H_2O/NH_3$/formaldehyde concentration determination was carried out using an FTIR analyzer downstream of the reactor. The inlet gas composition was similar to that typical for the Portable Life Support System (PLSS): ~20 ppm NH_3, ~0.5 ppm formaldehyde, ~ 1.0 vol.% CO_2, 29 vol.% O_2, and balance nitrogen. A more detailed description of this laboratory facility, experimental procedures, and selected previous results can be found in references [11–13].

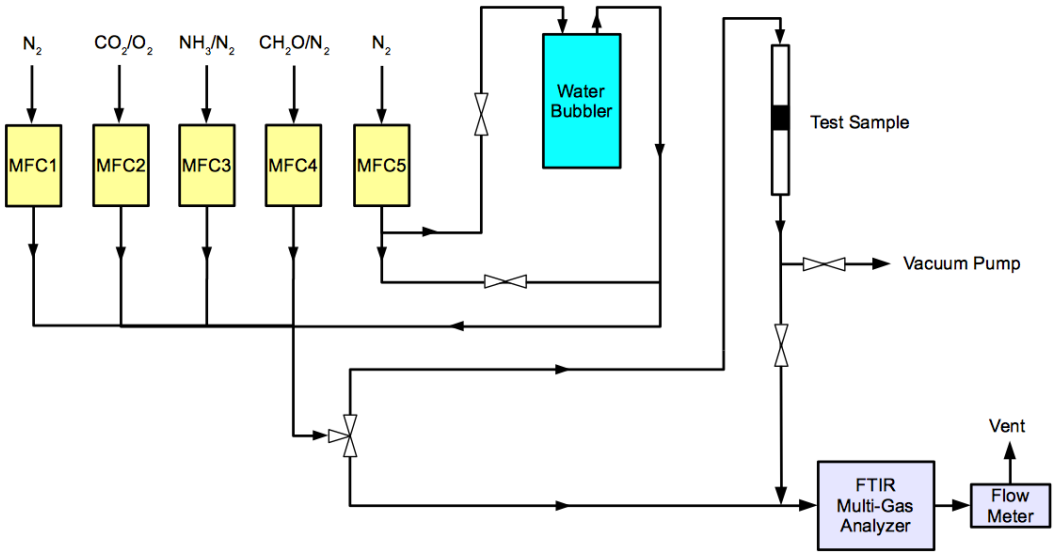

Figure 1. Sorption/desorption capacity test apparatus at AFR. MFC1 through MFC5 are mass-flow controllers. CH_2O is formaldehyde, which is supplied from a permeation-tube assembly.

III. Results and Discussion

A. Sorbent Fabrication and Characterization

1. Shape Retention During Carbonization

Samples of PC, PEI, and PEEK filaments were used in preliminary screening experiments to determine, qualitatively, the degree to which a given material could retain its shape upon carbonization.

Results of carbonization experiments performed using PEEK filaments, with and without carbon-fiber reinforcement, are shown in Figure 2 and Figure 3. The second polymer used was PEI. Many 3D-printing companies work with PEI, and this material is considered a high-performance polymer with good thermal resistance, although not as good as PEEK. A literature survey revealed that the carbonization yields of PEI are similar to those of PEEK (> 50 wt%), which makes PEI an attractive option to consider. Samples of carbon fiber reinforced PEI and PC filaments were used to evaluate their carbonization properties in terms of shape retention. It was found that PEI showed better shape retention than PC, but not as good as PEEK (see Figure 4).

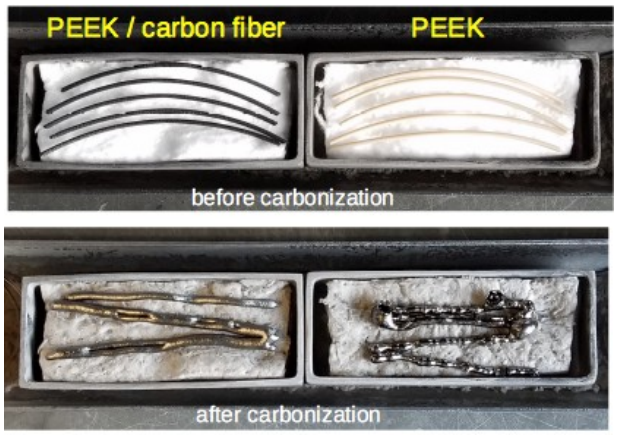

Figure 2. Carbonization of PEEK filaments at a final temperature of 800 °C and a heating rate of 5 K/min; carbon yield: 53.7 wt% of the original PEEK. Note that some filaments shifted upon handling and then fused.

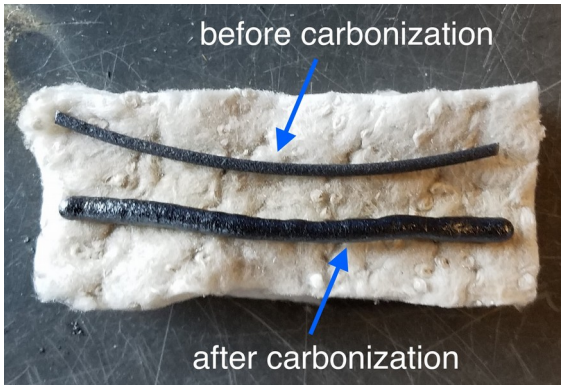

Figure 3. PEEK/carbon-fiber before and after insertion into a tube furnace preheated to 575 °C and holding at the above temperature for 30 minutes.

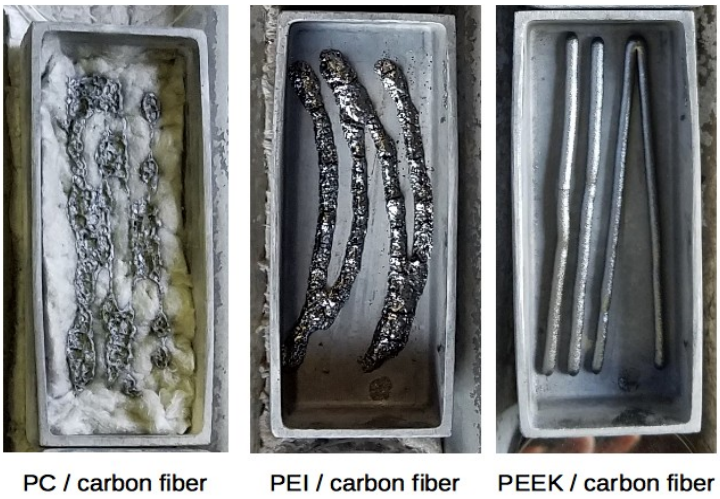

Figure 4. The comparison of post-carbonization shape retention characteristics of PC, PEI, and PEEK filaments reinforced with carbon fiber.

The following conclusions can be made on the basis of the above carbonization tests:

- Polymer/fiber filaments retain shape better than pure polymer filaments during carbonization (see Figure 2).
- PEEK appears to hold shape better than PEI, and much better than PC (see Figure 4).
- PEEK has a much higher carbon yield than PC (54 wt% and 14 wt%, respectively); also, higher than the carbon yield in PVDC carbonization (25 wt%), which was reported in previous studies.[10–27]
- The heating rate does not seem to have a strong effect on filament shape retention, at least for PEEK.

Ammonia and formaldehyde sorption and sorbent regeneration properties were later found to be excellent for the PEEK-based carbon, as discussed in section **III.B**. Consequently, carbon fiber reinforced PEEK (PEEK/CF) was selected for further work.

2. Monolith Design and Fabrication

The solid model of the 1 mm square channel monolith, with an 18-mm diameter, 6-mm height, a channel-wall thickness of 0.25 mm, and a 1-mm outer wall was created and used as a baseline design (see Figure 5). A square-channel geometry is quite typical for monoliths.[28] The inner channel and wall dimensions given above are expected to accommodate some swelling during carbonization, while still allowing gas to flow at rates that ensure low pressure drop across the monolith. Dimensional tolerances for the final product are still to be specified.

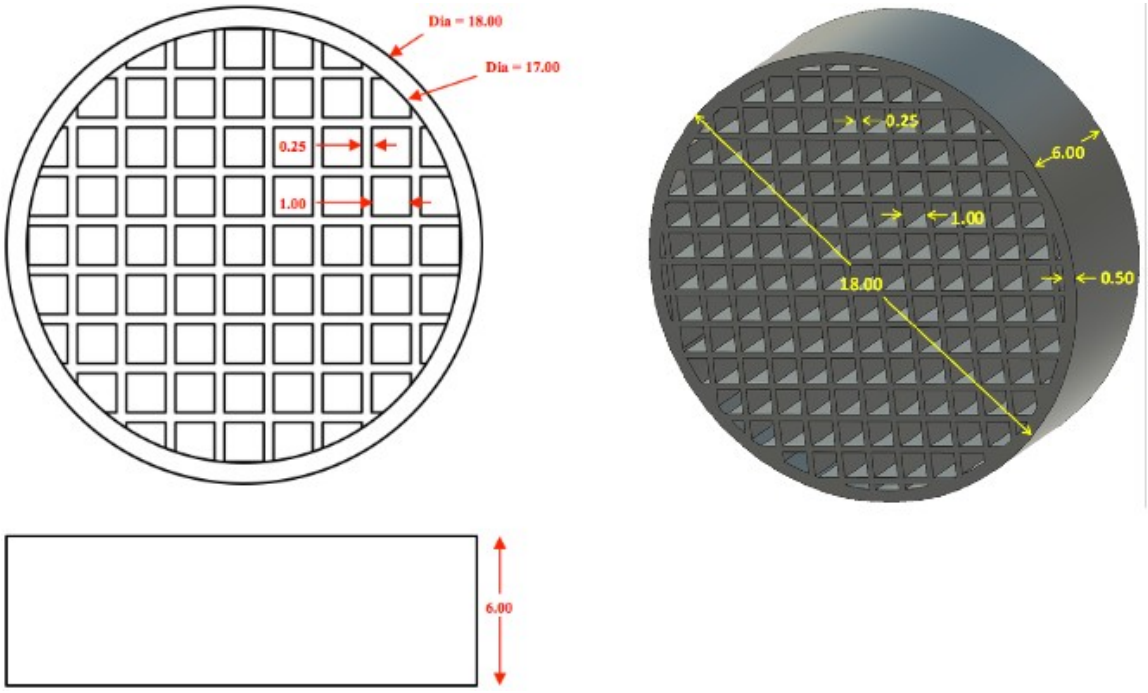

Figure 5. Baseline monolith design (not to scale); dimensions in millimeters.

Several companies that offer 3D-printing services were contacted for quotations on pieces fabricated from PEEK/CF. Two of them were short-listed, Cosine Additive and Vision Miner, and we ended up working with Vision Miner. We were surprised to find out that 3D printing using PEEK, but also carbon fiber reinforced PEEK, was far from straightforward. There were several challenges to overcome, such as nozzle plugging, and innovative modifications in the fabrication tooling and procedures had to be made. The use of PEEK without carbon-fiber reinforcement turned out to be particularly difficult, with a severe loss of overall monolith shape and channel structure was observed. This presumably occurred due to the localized melting caused by the hot injection nozzle.

A polymer monolith 3D printed using PEEK/carbon fiber filament with a target channel wall thickness of 0.25 mm is shown in Figure 6. It can be seen that the overall shape and channel structure is quite good. The channel walls are still thicker than prescribed, however, and some rounding of inside corners is evident. This is believed to be a result of the build-up of extra material from the sequential criss-cross deposition of continuous lines in the overlapping fashion.

To address the above issue, a new approach to printing the monoliths was developed (Figure 7a). In this technique, a single layer is formed by depositing a lattice of segmented lines in an alternating fashion. The next layer is deposited in the same way, but shifted to stagger the “breaks” from layer to layer. This approach minimizes the amount of the extra material, while maintaining the monolith strength. Square polymer monoliths (PEEK/CF) were printed using the modified deposition sequence. Figure 7b shows a single layer structure, and Figure 7c shows a multi-layer structure. A significant improvement in the channel shape and wall thickness is evident, as compared with Figure 6. Note that cylindrical shapes can be cut or machined from these square structures, or cylindrical designs can be developed.

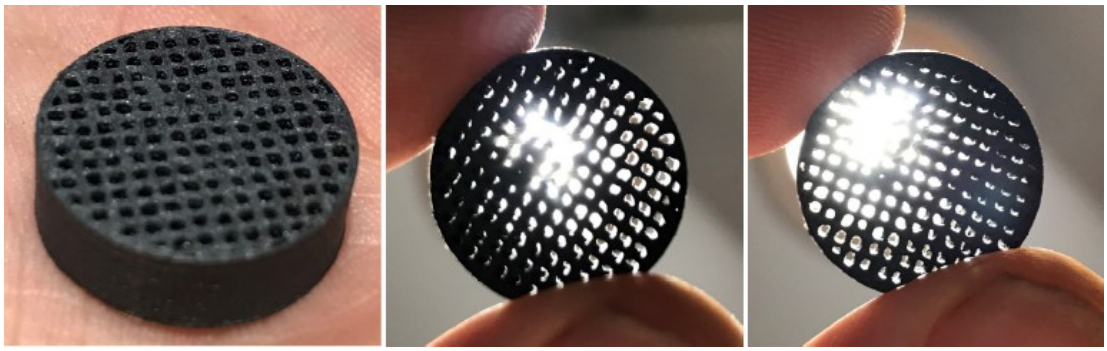

Figure 6. The polymer monolith printed using a PEEK/CF filament. The target wall thickness was 0.25 mm.

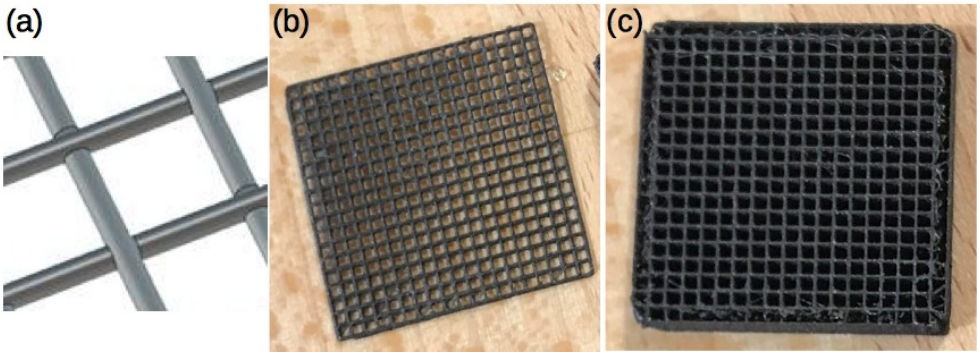

Figure 7. The polymer monolith printed using a PEEK/CF filament and a modified layer-deposition sequence: (a) the concept of depositing a lattice of segmented lines in an alternating fashion (a "log-cabin" approach); (b) a single-layer structure (monolith thickness, L = 0.5 mm); and (c) a multi-layer structure (monolith thickness, L = 3.0 mm). The target wall thickness was 0.25 mm.

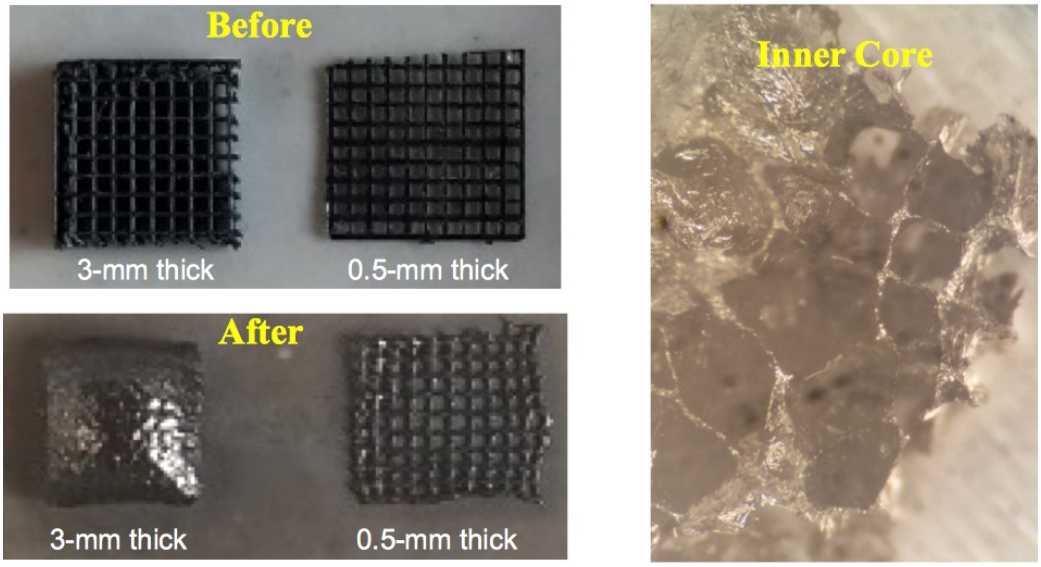

Figure 8. 3-mm and 0.5-mm thick test pieces carbonized at 800 °C. The thicker piece shows swelling and external "sealing" of channels. Some internal open cell structure is evident, however, in the thicker sample (see Inner Core).

Carbon fiber reinforced PEEK monoliths similar to the ones shown in Figure 7b and Figure 7c were carbonized, and it was found that shape retention was problematic in the case of 3.0-mm thick monoliths (Figure 8).

In order to understand the mechanism of polymer melting and carbonization during heat treatment, an experiment was designed in which the polymer sample was heated by an external furnace, while being visually observed through a mirror. It was found that PEEK monolith melting and fusion of channels took place in the temperature range 350–385 °C, with swelling observed at about 450 °C. A carbonization run was also performed using a thermogravimetric analyzer (TGA), which showed that the onset of devolatilization, indicated by sample weight loss, occurred well above 500 °C. Therefore, it is fair to conclude that melting happens before devolatilization, and this is why measures need to be taken to prevent the loss of monolith shape at the melting stage.

The above considerations led us to the idea of using support structures in the form of smooth, stainless-steel dowel pins inserted into monolith channels to prevent channel fusion during carbonization. The results for a 6-mm thick monolith are shown in Figure 9, where much better shape retention is observed than in Figure 8 for the 3-mm thick monolith.

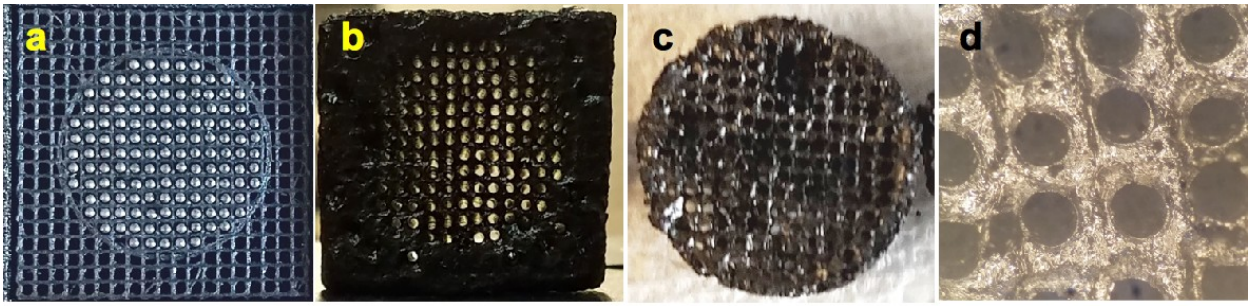

Figure 9. 1-mm square channel monolith (6-mm thick) carbonized at 800 °C: (a) monolith loaded with 0.8-mm diameter "support" stainless-steel pins prior to carbonization; (b) monolith after carbonization, with the pins removed; (c) trimmed monolith ready for adsorption testing; (d) a close-up of the channels now having a circular cross-section.

Since the use of individual support structures (pins) for each channel is tedious, an improved concept was put forward, in which two "beds of nails" are inserted into monolith channels from both ends of the monolith, as shown in Figure 10. The bed-of-nails approach would allow for the convenient manufacture of carbonized monolith sorbents, with the reusable bed-of-nails molds fabricated using 3D printing. The "nails" in each of the molds have a square cross-section to fit into the square channels, and they are tapered for easier removal after carbonization. This design will result in monolith channels that are also tapered in a staggered manner, as shown at the bottom of Figure 10.

The bed-of-nails approach was tested in our laboratory, and the results look promising, although some damage to the carbon monolith was observed due to the considerable roughness of the support elements ("nails"). This is shown in Figure 11. It turns out that the 3D printing process used in the fabrication of the top and bottom molds produces rough support structures, which results in strong adhesion of the carbonized material to the metal surface. The parts of the monolith that were not damaged, however, exhibit a nice regular pattern of tapered square channels, as shown in Figure 11c. It can certainly be concluded that the bed-of-nails concept has merit and warrants further investigation in the future. It is believed that the problem with metal surface roughness is manageable, and we are confident that improvements in the 3D printing technique will successfully resolve this difficulty.

Due to the time constraints, we had to defer further exploration of the bed-of-nails technique and use an improved method involving stainless-steel dowel pins for prototype fabrication instead. Since the dowel pins used in our early experiments (see Figure 9) experienced some lateral dislocation, we decided to constrain their motion by anchoring them at the top and the bottom using two support plates. The modified assembly is shown in Figure 12. It can be seen that, in addition to the top and bottom pin-support plates, there is a stainless-steel collar that encircles the 3D-printed PEEK/carbon-fiber monolith so that the polymer is well supported from all sides during the melting stage. The whole assembly is not gas tight, however, and the volatiles released during carbonization can freely escape from the carbon monolith.

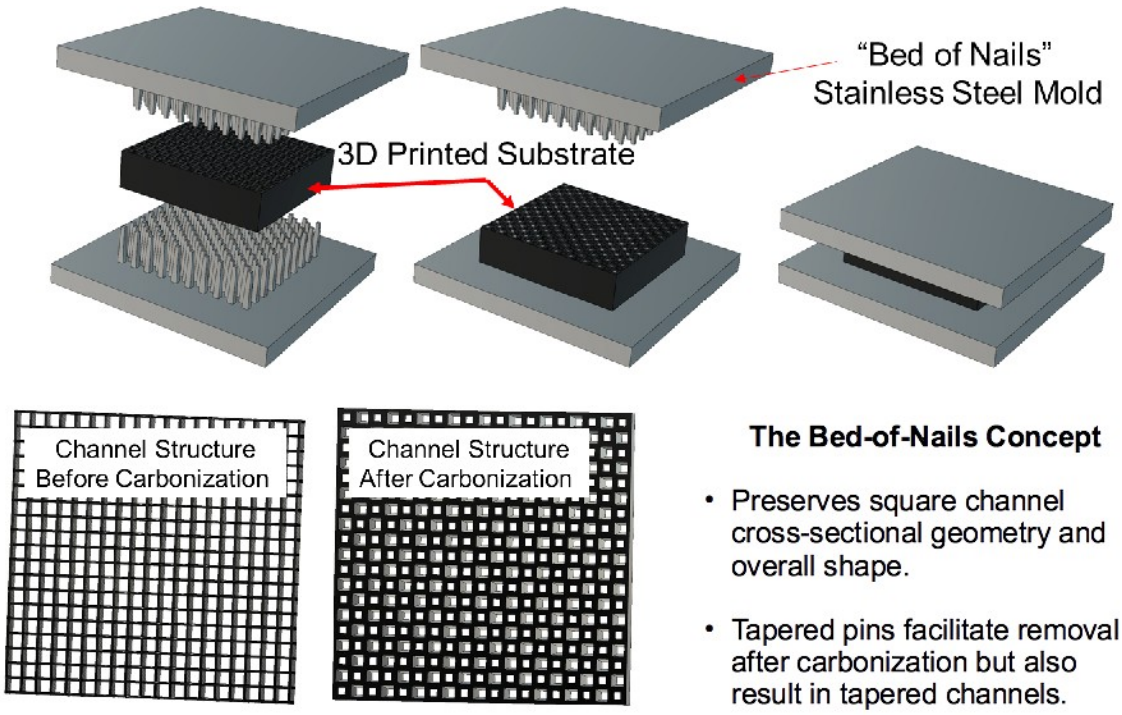

Figure 10. The "bed-of-nails" concept for improved shape retention during carbonization.

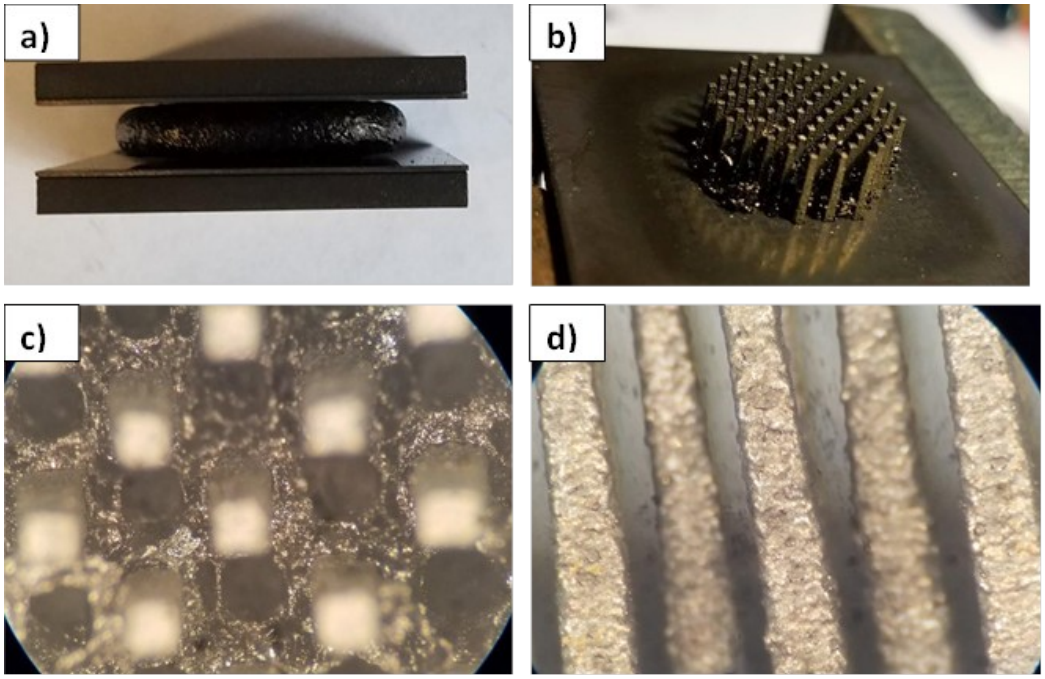

Figure 11. Carbonization with bed-of-nails supports: (a) bed-of-nails/monolith sandwich after carbonization; (b) carbonized monolith, partially destroyed after separation of upper and lower support forms; (c) channels observed in the remaining carbon; (d) close-up image of support pins showing high roughness.

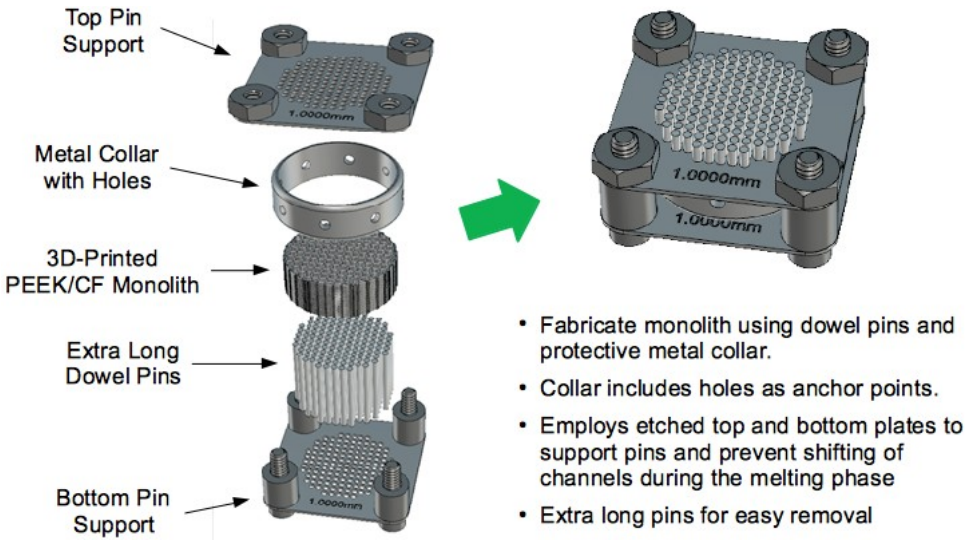

Figure 12. Concept for deliverable sub-scale prototype sorbent monolith fabrication.

3. Sub-Scale Prototype Sorbent Monolith Development

The assembly shown in Figure 12 was used to prepare a subscale prototype sorbent monolith, which is shown in Figure 13. It can be seen that the channels have a square cross-section prior to carbonization, whereas the carbonized monolith has round holes because round dowel pins were used. In the future, the use of the bed-of-nails technique will make it possible to preserve the original channel shape.

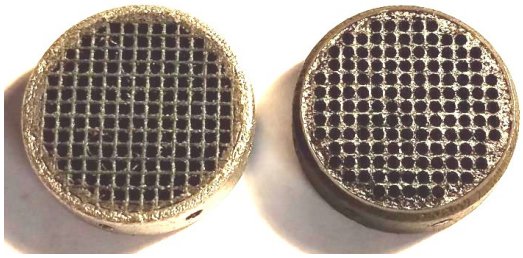

Figure 13. Deliverable sub-scale prototype carbon sorbent monolith before (left) and after (right) carbonization.

A subscale prototype sorbent assembly was put together using a sorbent monolith similar to the one shown in Figure 13, and it was subsequently delivered to NASA Johnson Space Center for further testing. Photographs of that unit are shown in Figure 14, and a brief description is given below.

The sorbent is an 18 mm diameter by 6 mm height monolith (inside a 20 mm OD metal collar) with an approximate mass of 0.35 g, excluding the metal collar. As shown, dabs of low vapor pressure adhesive (Torr Seal) are used to reinforce the monolith to the metal collar (both sides). The monolith/collar is secured inside a section of clear PVC tubing (20 mm ID x 25 mm OD) using the Torr Seal adhesive. Polypropylene tube adapters allow connections to ¼" OD tubing. The module is fully functional for testing at gas flow rates close to 1 L/min.

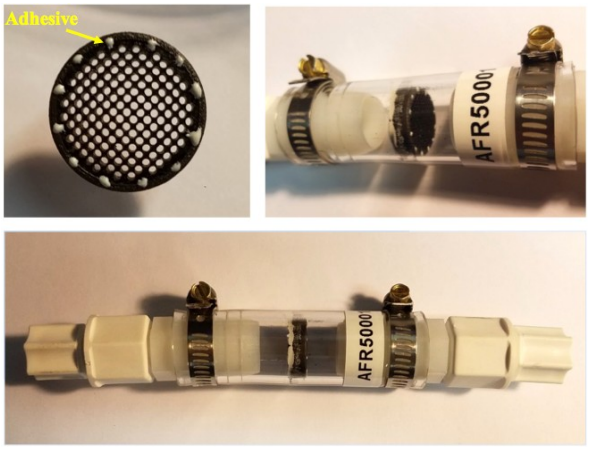

Figure 14. Images of the deliverable prototype sorbent test module. The top left photo shows the monolith with dabs of adhesive reinforcement to the metal collar. The top right and bottom photos show the monolith/test unit assembly.

4. Pore-Structure Characterization

Two samples of PEEK/CF-based sorbents were characterized with respect to their surface area, pore volume, and pore-size distribution using nitrogen-adsorption isotherms at 77 K. Both carbon sorbent monoliths were found to have similar pore-structure characteristics, and results for one of them are discussed below.

As expected, the carbon sorbent activated to ~18% weight loss (burn-off) is mostly microporous (70%

microporosity), i.e. having mainly pores smaller than 2 nm (20 Å), which is clearly seen in the pore-size distribution plot (Figure 15). The BET surface area, total pore volume, and micropore volume were found to be S_{BET} = 598 m^2/g, V_p = 0.312 cm^3/g, and V_{micro} = 0.217 cm^3/g, respectively. The above values are expressed per gram of carbon monolith, which contains both PEEK-derived carbon and about 21 wt% of the carbon-fiber reinforcement. (The original carbon-fiber content increases from ~10 wt% to ~21 wt% upon carbonization and activation, assuming that carbon fiber does not undergo devolatilization and activation.) Accounting for the presence of carbon fibers, the surface area, total pore volume, and micropore volume of the PEEK-carbon (exclusive of carbon fiber) were calculated to be: S^*_{BET} = 755 m^2/g, V^*_p = 0.394 cm^3/g, and V^*_{micro} = 0.274 cm^3/g, respectively.

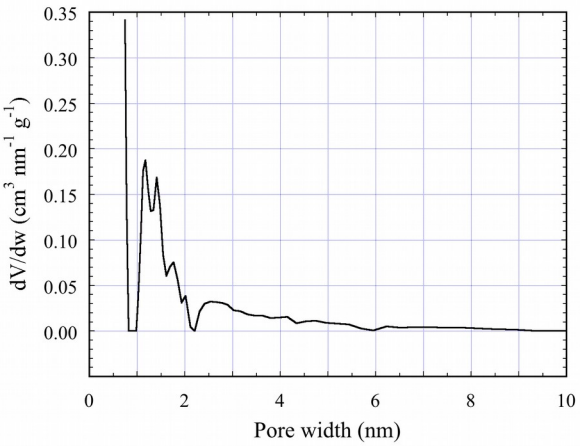

Figure 15. Pore-size distribution of PEEK/CF monolith (e.g., see Figure 8) carbonized at 800 °C, activated at 325 °C in air for 84 h to ~18 wt% burn-off. The data are derived from nitrogen isotherms at 77 K using the Functional Density Theory (DFT).

In our previous work,[13] we developed a correlation between the ammonia sorption capacity of PVDC-carbons and their pore volume, ΔV_2, in the range of pore widths 0.9–2.2 nm. It would be interesting to see how the ammonia-sorption performance of PEEK-carbons compares with data for PVDC-carbons, and this will be studied in some detail in our future work. At the present time we are able to add a single data point for the PEEK/CF-derived carbon to our old PVDC-carbon data, and the result is shown in . Although no firm conclusions can be drawn on the basis of a single data point, it certainly appears that the PEEK-carbon performs in a similar way as PVDC-carbons having similar relevant pore-structure characteristics (ΔV_2).

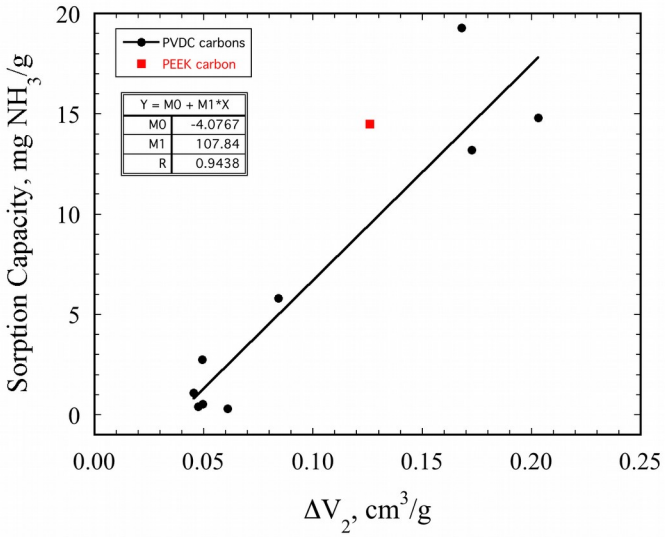

Figure 16. Ammonia-sorption capacity versus ΔV_2, the volume of pores in the range 0.9–2.2 nm for a PEEK-carbon (red marker) and for PVDC-carbons (black markers). PVDC-carbon data from ref. [13].

5. XPS Data

X-Ray Photoelectron Spectroscopy (XPS) analysis was used to gain insights into the carbon surface chemistry and the relative changes produced by carbon activation and exposure to ammonia. The analysis was performed by Rocky Mountain Laboratories, Inc. of Golden, Colorado. The following three PEEK/CF samples were analyzed for relative amounts of carbon, oxygen, and nitrogen, and also for the functional groups present on the carbon surface:

- *(C)* – PEEK/CF carbonized at 800 °C
- *(C+A)* – PEEK/CF carbonized, and then activated in a flow of air
- *(C+A+NH₃)* – PEEK/CF carbonized, activated, and exposed to NH_3

Results are shown in Table 1, and they indicate that carbon activation introduces oxygen functionalities onto carbon surface, and also that carbon exposure to ammonia results in the formation of nitrogen functionalities on the surface. The speciation of nitrogen functionalities for sample C + A + NH_3 is given in Figure 17. It can be seen that nitrogen is associated with oxygen in the N-C=O and N-(COO) functionalities, which is consistent with the strong enhancement of ammonia sorption capacity by surface oxidation.[10,11] Since samples subjected to XPS analysis are outgassed in high

Table 1. Relative elemental composition (atom %); see text for sample identification.

Sample	C	O	N
C	96.1	3.9	–
C + A	84.3	15.7	–
C + A + NH_3	83.5	15.5	1.0

vacuum, only the species that are strongly (irreversibly) bound can be analyzed. Thus, there is evidence that some irreversibly bound ammonia is present on the carbon surface, but the amount of such species is likely much lower than in the case of activated carbons derived from coal, coconut shells, and other organic precursors that, in contrast to polymer-derived carbons, contain appreciable amounts of impurities. In the case of acid-impregnated activated-carbon, the amount of irreversible ammonia is certainly even larger, as evidenced by the poor regenerability of such carbons reported in the review paper by Paul and Jennings[9].

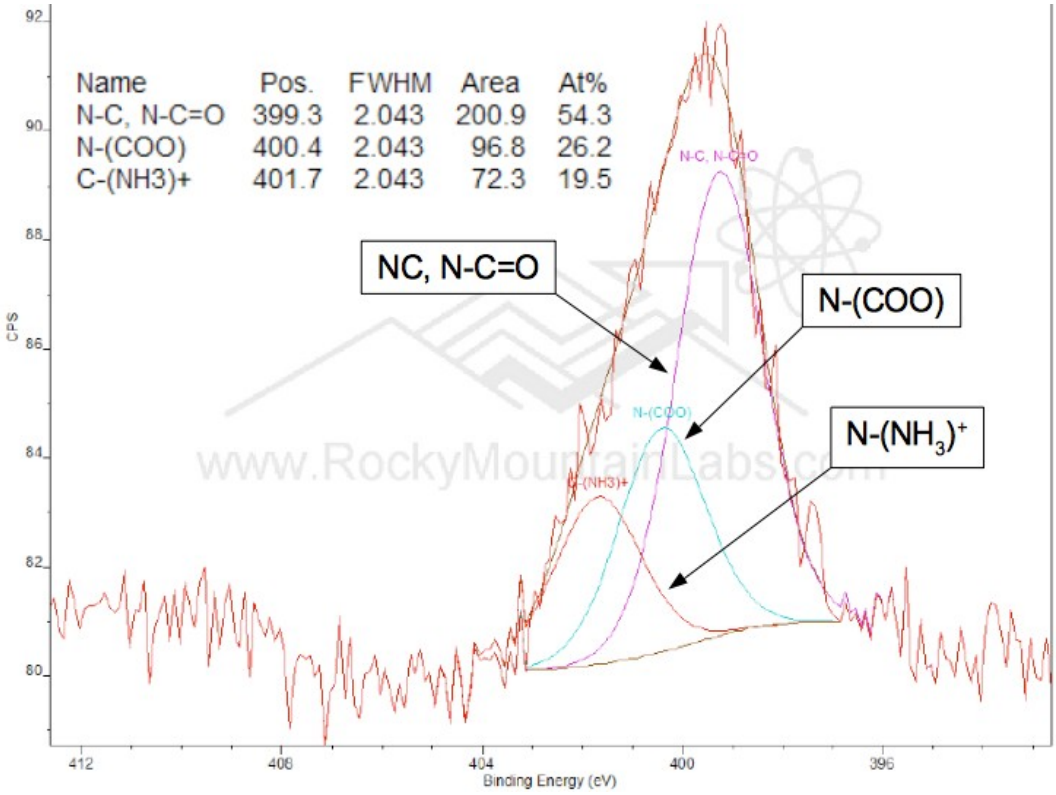

Figure 17. XPS data for carbonized and activated PEEK/CF sample exposed to ammonia (C + A + NH_3).

B. Sorbent Testing

1. Ammonia and Formaldehyde Sorption and Sorbent Regeneration

Ammonia Sorption on Granular Sorbents – Several PEEK/CF granular sorbents were prepared using the carbonization and mild-oxidation (activation) techniques described in references.[11] Samples of these carbons, which had different degrees of oxidation burn-off, were used to determine the equilibrium ammonia sorption capacity at room temperature. These data were then compared with results of our previous work on PVDC-based sorbents,[13] and this comparison is shown in Figure 18. It can be seen that the sorbents derived from the PEEK/CF filament perform as well as the PVDC-based sorbents, which actually exceeded our expectations, especially that no sorbent optimization was attempted.

Regeneration of Sorbents Supported on Reticulated Carbon Foam – A test sample was produced by impregnating reticulated carbon foam with pure PEEK powder, followed by carbonization and low temperature oxidation, as described in ref. [11] After the initial ammonia-sorption test, regeneration was performed by exposing the sample to high vacuum (ultimate vacuum ~ 5 x 10^{-6} Torr) for 6 hours. Slightly better than 50% regeneration was achieved (Figure 19), which is consistent with previous results obtained with PVDC-derived carbon samples of the same form.[11] Thus, it is fair to conclude that PEEK/CF is a promising material for monolithic TC sorbents in terms of: (1) shape retention upon carbonization; (2) ammonia sorption; and (3) vacuum regeneration.

Ammonia Sorption and Sorbent Regeneration for Carbon Monoliths – Several equilibrium sorption experiments were performed using carbon monoliths. Data presented in Figure 20 were collected on the same sample subjected to four sorption-regeneration cycles. Vacuum regeneration was performed at room temperature by removing the sorbent from the test cell and placing it in a high-vacuum chamber for six hours (typically reaching ~0.9 x 10^{-7}

Torr). The gas flow rate of 1.0 L/min was used, and the gas composition was: 20 ppm NH_3, 1.0 vol.% CO_2, 29 vol.% O_2, and balance nitrogen in Cycles 1–3, and additionally 3 ppm formaldehyde in Cycle 4. As in the case of granular sorbents, slightly better than 50% regeneration was achieved in Cycle 1, and the sorption capacity was found to stay unchanged in Cycles 2–4. This behavior is consistent with our prior work on PVDC carbon sorbents.[11]

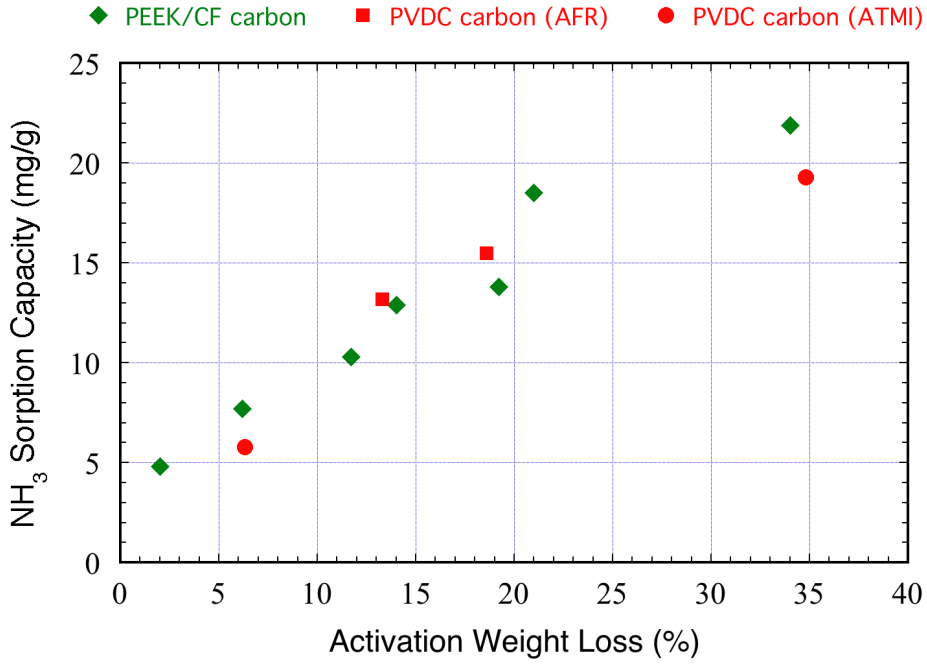

Figure 18. Ammonia-sorption capacity (mg NH_3/g carbon sorbent) versus oxidation weight loss for granular carbons derived from PEEK/CF (green) and PVDC (red). (Red squares are for granules carbonized at AFR and red circles are for granules carbonized at Entegris.) Note that the measurements for the PEEK/CF do not account for the presumed parasitic weight of the carbon fibers, but this effect is small as carbon fibers constitute only ~10 wt% of the PEEK/CF filament. PVDC-carbon data from ref. [13].

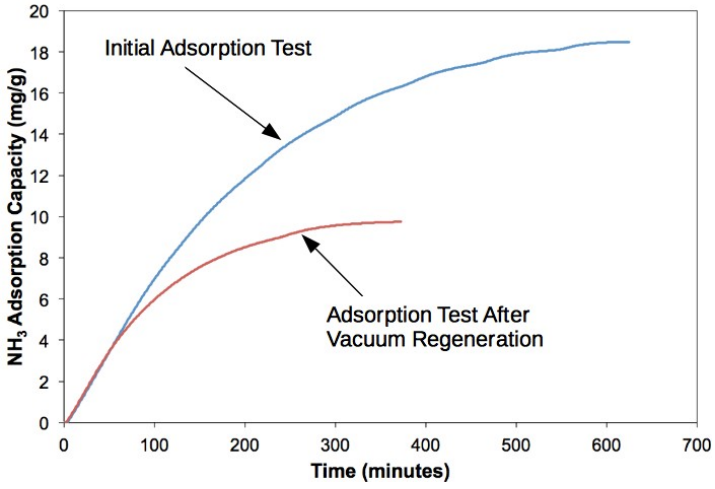

Figure 19. Ammonia-sorption capacity for the PEEK/CF-based sorbent before and after vacuum regeneration.

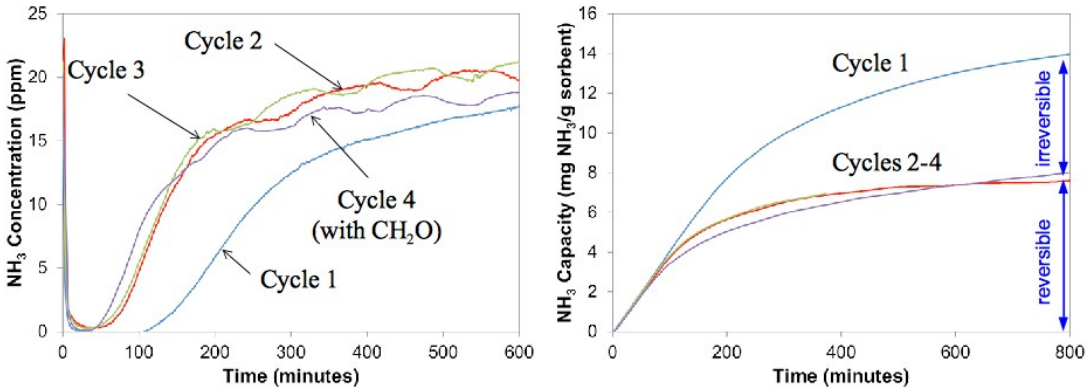

Figure 20. Ammonia sorption and sorbent regeneration cycles for a PEEK-based carbon monolith. Breakthrough curves are shown on the left, and the corresponding sorption-capacity curves on the right. Relative amounts of reversibly and irreversibly bound ammonia are indicated in the sorption-capacity curves. The inlet-gas composition was: 20 ppm NH_3, 1.0 vol.% CO_2, 29 vol.% O_2, and balance nitrogen in Cycles 1–3, and additionally 3 ppm formaldehyde in Cycle 4. All experiments were performed under dry-gas conditions.

The Effect of Humidity on Ammonia Sorption – An additional experiment, i.e. Cycle 5, was performed using the same sorbent discussed in the previous section. This time, the gas composition was the same as in Cycle 4, except a relative humidity of 40% was used. Data in Figure 21 show that the presence of water in the inlet gas leads to enhanced ammonia sorption by a factor of two. This is presumably due to the additional ammonia capture by dissolution in the aqueous phase adsorbed on the monolith. The above result is in agreements with our previous work on PVDC-based carbons.[11]

Formaldehyde Sorption – Figure 22 shows breakthrough and sorption-capacity curves for formaldehyde adsorption on a PEEK-based carbon monolith. It can be seen that, under conditions used in this experiment, the breakthrough never occurs, which means that all the formaldehyde present in the inlet gas gets adsorbed. The test had to be aborted after more than 1,000 minutes (~17 hours) of excellent sorbent performance.

Ammonia Sorption under Rapid-Cycling Conditions – The large ammonia equilibrium sorption capacity demonstrated by our PEEK-carbon monoliths (up to 20 mg NH_3 per gram of sorbent) is certainly an attractive feature of our technology. The fact that multiple adsorption-desorption cycles can be performed without sorption-capacity degradation, except for Cycle 1, as discussed above, is also encouraging. What these experiments do not reveal, however, is desorption kinetics, which are of paramount importance if the preferred mode of operation is rapid cycling with a frequency of several minutes.

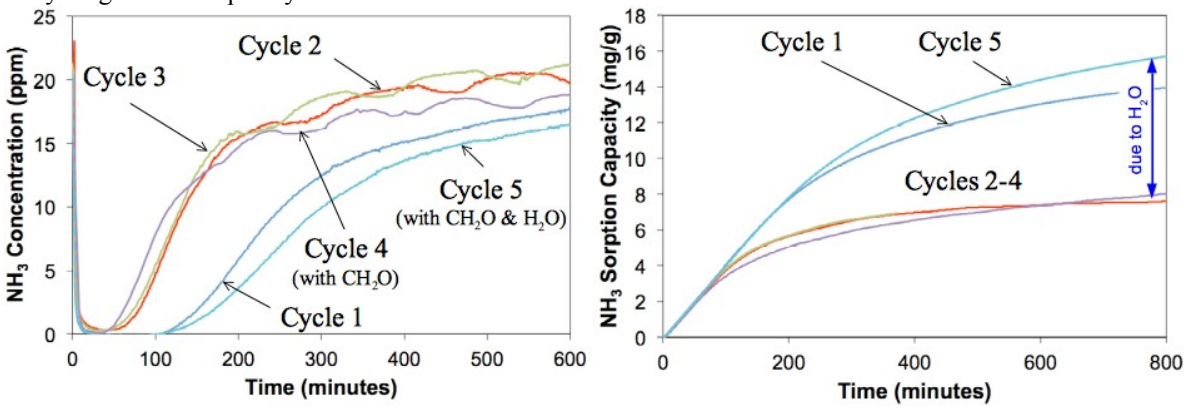

Figure 21. Ammonia sorption and sorbent regeneration cycles for a PEEK-based carbon monolith under dry-gas (Cycles 1-4) and humid-gas (Cycle 5) conditions. Breakthrough curves are shown on the left, and the corresponding sorption-capacity curves on the right. The inlet-gas composition was: 20 ppm NH_3, 1.0 vol.% CO_2, 29 vol.% O_2, and balance nitrogen in Cycles 1–3, additionally 3 ppm formaldehyde in Cycle 4, and additionally 3 ppm formaldehyde and water at a relative humidity of 40% in Cycle 5.

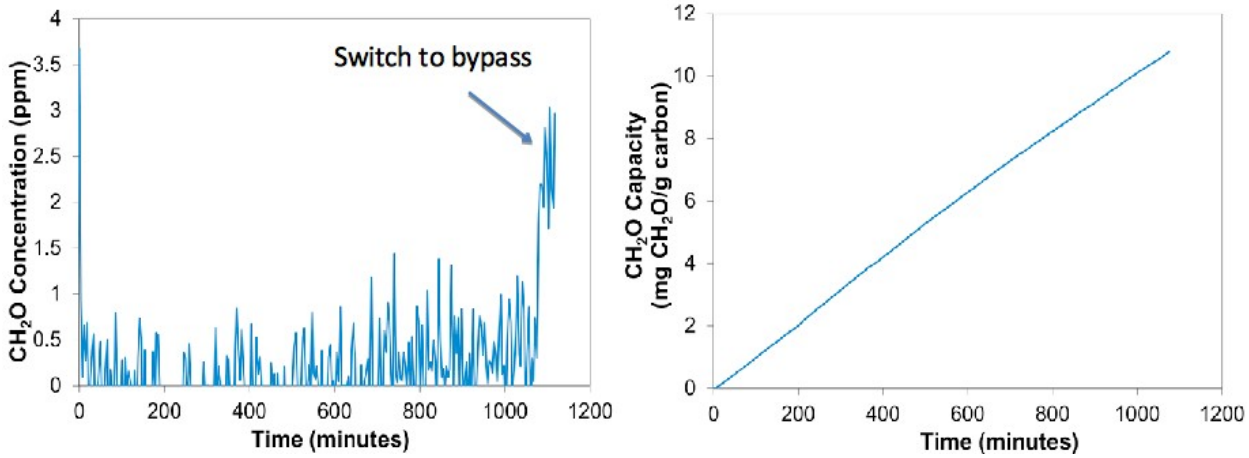

Figure 22. Formaldehyde adsorption on PEEK/carbon-fiber carbon monolith. The inlet-gas composition was: 3 ppm formaldehyde, 20 ppm NH_3, 1.0 vol.% CO_2, 29 vol.% O_2, and balance nitrogen.

In order to evaluate the suitability of PEEK-carbon monoliths for rapid cycling pressure swing operation, the following experiment was carried out. A carbon monolith derived from PEEK/CF was exposed to a flow of 20 ppm ammonia over more than 18 hours to reach the state of complete sorbent saturation with ammonia. The sorbent was then subjected to rapid sorption-desorption cycles, with each adsorption and desorption step taking 5 minutes. The gas flow rate was 1.0 L/min, and the carbon weight was 0.25 g. Vacuum regeneration (desorption) was performed using a roughing pump capable of providing only ~0.35 Torr vacuum at the sample location during the pumpdown. This of course was far from ideal, but the objective of this experiment was to see if the sorbent's response was fast enough, even though its sorption performance may have been reduced due to the poor vacuum.

Results are shown in Figure 23, and they actually look quite impressive, especially in view of the poor-quality vacuum used. The sorbent response is rapid, with the outlet ammonia concentration dropping from 20 ppm to 5 ppm in each adsorption cycle under steady-state conditions. The first few cycles show worse performance, and this is almost certainly due to the fact that the initial sorbent condition is full saturation. It simply takes a few cycles for the inventory of the adsorbed ammonia to be cleared from the carbon surface by the action of the roughing pump. This transient operation does not take long, and the sorbent soon reaches what appears to be a stable steady-state operation.

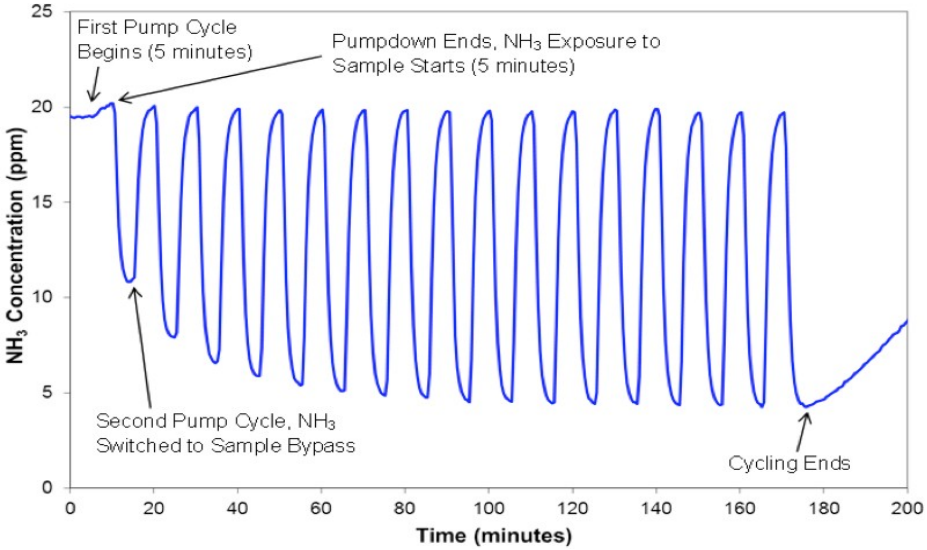

Figure 23. Rapid-cycle testing of a PEEK-carbon sorbent monolith using a roughing pump with a vacuum of ~0.35 Torr. The sorbent weight used was 0.25 g, and the gas flow rate was 1.0 L/min.

The effect of improved vacuum quality on sorbent performance was addressed in a separate experiment, and results of the fast cycle regeneration test that was conducted under improved vacuum conditions are shown in Figure 24. The sample (carbon mass ~ 0.25 g) was the same monolith that was tested at ~0.35 Torr conditions (see Figure 23). As before, the sample was re-saturated by exposure to 20 ppm NH_3 (in CO_2/O_2 and N_2) at 1 L/min for more than 18 hours. Regeneration was performed by transferring the sample to a high-vacuum chamber (estimated volume ~2 ft^3) fitted with a turbomolecular pump/rotary vane pump system. The regeneration period was 5 minutes and consisted of 3 steps: (1) an initial chamber rough pumpdown to 0.3 Torr using the rotary pump (~1.5 min); (2) turning on the turbopump for a period of ~3 minutes; and (3) shutdown of the pump system and dry air backfill (~30 s). Under these conditions, the sample was actually exposed to high vacuum for less than 3 minutes, and the lowest vacuum levels achieved were only ~4×10^{-5} Torr. The sample was then transferred back to the test station and immediately re-exposed to 20 ppm NH_3 at 1 L/min for 5 minutes. The transfer period to and from the pump station was ~1.5 minutes, which accounts for the total apparent cycle period (exposure plus regeneration) of ~13 minutes seen in the data. It is assumed that regeneration at ambient conditions during the transfer period was negligible.

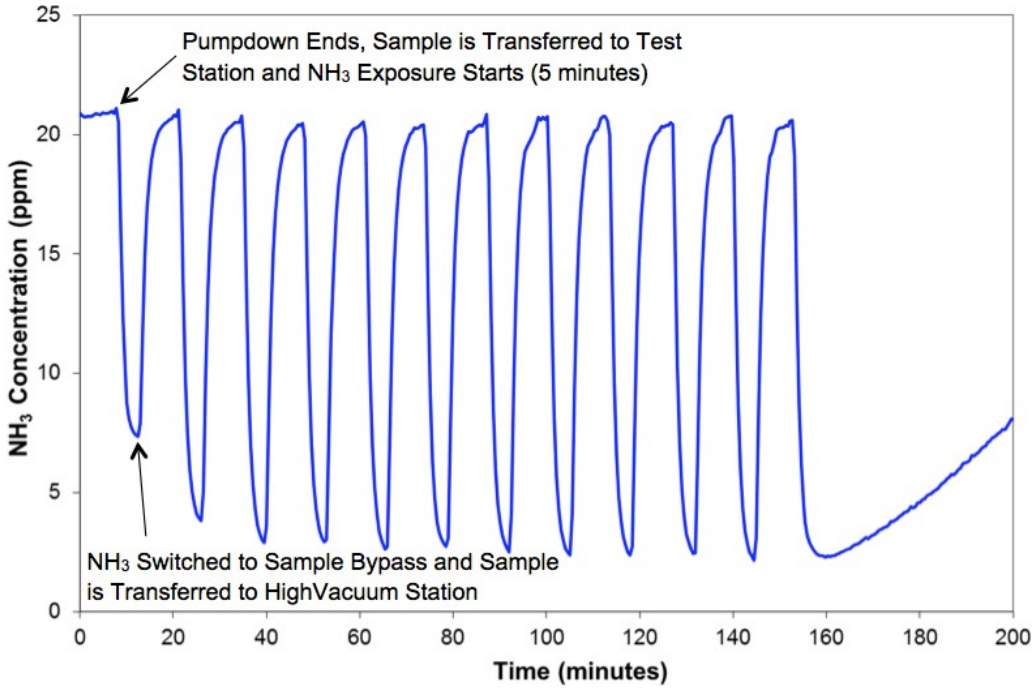

Figure 24. Rapid-cycle testing of a PEEK-carbon sorbent monolith using regeneration in a high-vacuum station (~4×10^{-5} Torr). The sorbent weight used was 0.25 g, and the gas flow rate was 1.0 L/min.

General observations are as follows:

- The vacuum system that was employed for regeneration was not ideal for these tests. Its ability to provide high vacuum pumping was hampered by the large chamber volume, causing the relatively long roughing and backfill periods. In future work, the high vacuum equipment will be directly attached to the test station and pumping volumes will be minimized for faster pumpdown with improved vacuum quality.
- Despite the limitations of the apparatus that was employed, a significant improvement in the ammonia knockdown was achieved, reaching concentrations lower than 2.5 ppm at the outlet.

In future research, we are planning to test our sorbents over hundreds of cycles, and, as stated above, we are going to use much better vacuum. At this stage, it is fair to conclude that the currently availbale data demonstrate the feasibility of using PEEK-carbon monoliths for pressure-swing operation with cycle times of a few minutes.

2. Pressure Drop

One of the main advantages of the monolithic structure is a low pressure drop, which also means a low fan-power requirement. To get an idea about the magnitude of the pressure drop across the sorbent monolith, calculations were performed using the approach described by Cybulski and Moulijn (1994).[28] Input information is

summarized in Figure 25, and based on these design parameters, monolith characteristics can be calculated, as described below.

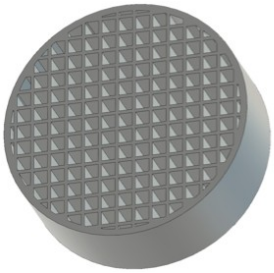

- Channel size, d = 1 mm
- Diameter, D = 18 mm
- Number of channels, N = 141
- Monolith height, L = 6 mm
- Wall thickness, δ_w = 0.25 mm
- Outer wall thickness, δ_{ow} = 0.50 mm
- Air flow rate: 1 L/min
- Air temperature: 30 °C

Figure 25. Input parameters for pressure-drop calculations.

Monolith voidage, ε (-): $\epsilon = \frac{D^2}{(D+\delta_w)^2} = 0.64$

Cell density, n (cells per square inch): $n = \frac{1}{(D+\delta_w)^2} = 413$

Hydraulic diameter, D_H (cm): $D_H = \frac{\sqrt{\epsilon}\,\delta_w}{(1-\sqrt{\epsilon})} = 0.10$

Geometric surface area per unit volume, σ (cm^2/cm^3): $\sigma = \frac{4|\sqrt{\epsilon}-\epsilon|}{\delta_w} = 25.6$

The pressure drop can now be computed using the Darcy-Weisbach equation:

$$\Delta p = 4 f \frac{L}{D_H} \rho \frac{u^2}{2} \qquad (1)$$

where Δp is the pressure drop, f is the friction factor, ϱ and u are gas density and velocity, respectively. The friction factor for monoliths with square channels can be calculated as follows[29,30]:

$$4f = \frac{56.92}{\mathrm{Re}}\left(1+0.0445\,\mathrm{Re}\frac{D_H}{L}\right)^{0.5} \qquad \mathrm{Re} = \frac{u D_H \rho}{\mu} \qquad (2)$$

where Re is the Reynolds number and μ is gas viscosity.

Using the properties of air at 30 °C, the above expressions can be used to calculate the pressure drop as:

$$\Delta p = 0.374\,Pa = 0.003\,Torr = 0.002\ \mathrm{in}\,H_2O = 0.000\,psi$$

As expected, this pressure drop is immeasurably small.

Although no meaningful measurements of such a low pressure drop could easily be performed, we did carry out pressure-drop measurement at much higher flow rates. The flow resistance was determined using a small system previously described.[11] The gas flow rate was measured by a flow meter, and pressure gauges were used to determine pressure upstream and downstream of the sorbent element.

Results presented in Figure 26 show that monolithic sorbents will indeed have a tremendous advantage over granular ones, which will lead to significant savings in fan-power demand. In agreement with the calculations presented above, the pressure drop at 1 L/min is negligibly small. System scale-up and pressure drop in a full-scale Trace Contaminant Control System (TCCS) will be addressed in future work.

3. Mechanical Strength

One of the shortcomings of granular carbon sorbents currently used for TC control is attrition and the release of fine particles, which may take place due to vibrations occurring during spacecraft launch. It is expected that carbon monoliths will exhibit better resistance to vibrations, but this needs to be demonstrated. A preliminary evaluation of the mechanical integrity of a prototype test unit subjected to vibration was performed using a laboratory sieve shaker (CSC Scientific model no. 18480). The test cell was clamped directly to the shaker stage and shaken for a period of 5 minutes at an intermediate setting of 5 on the sieve shaker. Photographs of the test cell taken before and after the shake test revealed no evidence of damage to the carbon monolith, such as fracture or shedding. Although the above test is not directly linked to any standard testing methodology, it nonetheless provides indirect proof of mechanical robustness of our sorbents. More extensive and rigorous testing will be performed in the next phase of the project.

4. Carbon Flammability Test

A simple, preliminary flammability test was performed to ensure the developed carbon sorbents do not pose fire hazards. The approach to flammability testing is based on a TGA experiment in which a sample of carbon sorbent is heated in a flow of pure oxygen at 10 K/min to see at what temperature the carbon starts losing weight due to oxidation. The sorbent monolith sample used in this test was derived from carbon fiber reinforced PEEK, which was first carbonized in a flow of nitrogen at 800 °C, and subsequently activated in a flow of air at 325 °C to a burn-off of ~18 wt%. Results of the above test are presented in Figure 27, and they show that no significant oxidation takes place below 350 °C on a time scale of 1-2 hours. These data indicate good PEEK carbon's resistance to oxidation.

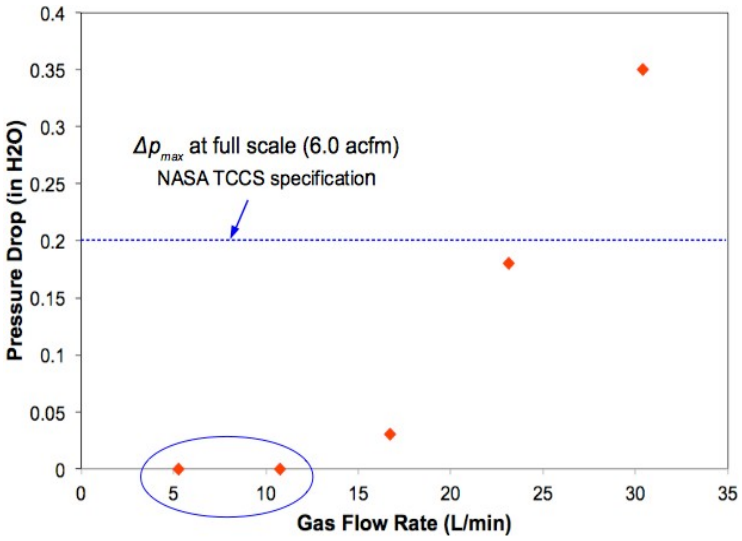

Figure 26. Pressure drop measurements for an 18-mm diameter, 6-mm high PEEK-carbon sorbent. The pressure drop is negligibly small for this sorbent geometry for flow rates below 10 L/min.

Even though PEEK-carbon activation in a flow of air at 325 °C is associated with some weight loss, this activation process is extremely slow, occurring on a time scale of more than 80 hours to reach the weight loss of 18 %. Thus, it can be concluded that the PEEK-based sorbent is unlikely ever to become a fire hazard due to the extremely slow oxidation kinetics at temperatures well below 300 °C.

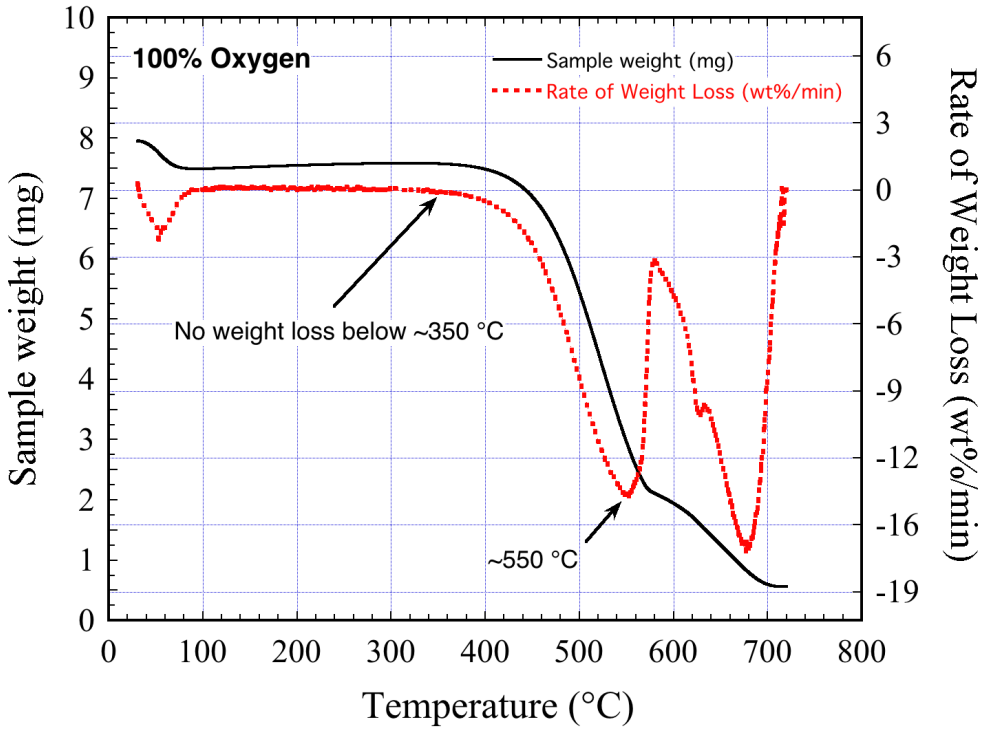

Figure 27. Carbon-flammability test: PEEK / carbon fiber carbonized at 800 °C and activated to a burn-off of ~18 wt%. The TGA experiment was carried out in a flow of 100% oxygen at a heating rate of 10 K/min.

IV. Conclusions

The technical feasibility of using 3D printing to fabricate polymer monoliths with multichannel geometry was demonstrated. The carbon fiber reinforced PEEK polymer was successfully used for this purpose. The above polymer monoliths were subsequently carbonized and activated to form microporous carbon monolith TC sorbents with good shape retention and mechanical strength.

Excellent ammonia and formaldehyde capture and rapid vacuum sorbent regeneration, on a time scale of 5 minutes, was demonstrated. The results of this study were found to be consistent with our previous work on PVDC-carbons,[11,14] and also showed that PEEK-carbons are competitive with respect to the current state of art (oversized, expendable, acid-impregnated granular activated carbon). More specifically, reproducible regeneration by exposure to vacuum at room temperature was demonstrated throughout multiple adsorption-desorption cycles. Ammonia-sorption capacity was found to be up to 20 mg NH_3 per gram of sorbent, depending on sorbent preparation conditions. Ammonia-sorption capacity usually dropped after the first cycle, but then remained constant over multiple cycles. Under the condition used in this study, formaldehyde sorption was found to be so good that formaldehyde breakthrough did not occur for at least 17 hours.

A subscale sorbent prototype was designed, constructed, and delivered to NASA Johnson Space Center.

Acknowledgments

Financial support for the project was provided by NASA SBIR program under Contract No. 80NSSC18P1961. 3D-printed monoliths were fabricated by Vision Miner. Nitrogen-adsorption and XPS analyses of carbon samples were performed by Dr. Indrek Külaots of Brown University and by Rocky Mountain Laboratories, respectively. Helpful discussions and consulting input were provided by Professor Eric Suuberg of Brown University, and Julia M. Worrell of NASA Johnson Space Center contributed thoughtful guidance and discussions. The above contributions are gratefully acknowledged.

References

[1] Rouquerol, J., Avnir, D., Fairbridge, C. W., Everett, D. H., Haynes, J. M., Pernicone, N., Ramsay, J. D. F., Sing, K. S. W., and Unger, K. K., "Recommendations for the characterization of porous solids (Technical Report)," *Pure and Applied Chemistry*, **66**(8), 1739–1758, 2009

[2] Birbara, P. J., Filburn, T. P., and Nalette, T. A., "United States Patent: 5876488 - Regenerable solid amine sorbent," US Pat. No. 5876488, 1999

[3] Filburn, T., Nalette, T., and Graf, J., "The Design and Testing of a Fully Redundant Regenerative CO2 Removal System (RCRS) for the Shuttle Orbiter," *Proc. 31st Int. Conf. on Environmental Systems (ICES)*, SAE International, Orlando, Florida, 2001-01–2420, 2001

[4] Monje, O., Brosnan, B., Flanagan, A., and Wheeler, R. M., "Characterizing the adsorptive capacity of SA9T using simulated spacecraft gas streams," *Proc. 40th Int. Conf. on Environmental Systems (ICES)*, Barcelona, Spain, AIAA-2010-6063, 2010

[5] "NASA SBIR and STTR 2016 Program Solicitations | NASA SBIR & STTR Program Homepage," <https://sbir.nasa.gov/solicit-detail/56329>, n.d. (Mar. 9, 2018)

[6] Monje, O., Nolek, S. D., and Wheeler, R. M., "Ammonia offgassing from SA9T," *Proc. 41st International Conference on Environmental Systems (ICES)*, Portland, Oregon, AIAA-2011-5101, 2011

[7] Button, A. B., Sweterlitsch, J. J., Broerman, C. D., and Campbell, M. L., "Trace contaminant testing with the Orion atmosphere revitalization technology," *Proc. 40th Int. Conf. on Environmental Systems (ICES)*, Barcelona, Spain, AIAA-2010-6299, 2010

[8] Paul, H. L., Jennings, M. A., and Waguespack, G. M., "Requirements and sizing investigation for Constellation space suit Portable Life Support System Trace Contaminant Control," *Proc. 40th Int. Conf. on Environmental Systems*, AIAA, Barcelona, Spain, Paper No. AIAA 2010-6065, 2010

[9] Paul, H. L., and Jennings, M. A., "Results of the trace contaminant control trade study for space suit life support development," *Proc. 39th Int. Conf. on Environmental Systems*, SAE International, Savannah, Georgia, Paper No. 2009-01-2370, 2009

[10] Wojtowicz, M. A., Cosgrove, J. E., and Serio, M. A., "Carbon sorbent for reversible ammonia sorption," US Pat. No. 9,073,039, 2015

[11]Wójtowicz, M., Cosgrove, J., Serio, M., and Jennings, M., "Reversible Ammonia Sorption on Carbon for the Primary Life Support System (PLSS)," *Proc. 42nd International Conference on Environmental Systems*, American Institute of Aeronautics and Astronautics, San Diego, California, AIAA-2012-3437, 2012

[12]Wójtowicz, M. A., Cosgrove, J. E., Serio, M. A., Manthina, V., Singh, P., and Chullen, C., "Carbon-Based Regenerable Sorbents for the Combined Carbon Dioxide and Ammonia Removal for the Primary Life Support System (PLSS)," *Proc. 44th International Conference on Environmental Systems (ICES)*, Tucson, Arizona, ICES-2014-241, 2014

[13]Wójtowicz, M. A., Cosgrove, J. E., Serio, M. A., and Wilburn, M. S., "Adsorption of ammonia on regenerable carbon sorbents," *Proc. 45th International Conference on Environmental Systems (ICES)*, Bellevue, WA, Paper No. ICES-2015-179, 2015

[14]Wójtowicz, M. A., Cosgrove, J. E., Serio, M. A., and Wilburn, M. S., "Co-adsorption of Ammonia and Formaldehyde on Regenerable Carbon Sorbents for the Primary Life Support System (PLSS)," *Proc. 46th International Conference on Environmental Systems (ICES)*, Vienna, Austria, Paper No. ICES-2016-345, 2016

[15]Wójtowicz, M., Florczak, E., Kroo, E., Rubenstein, E., Serio, M. A., and Filburn, T., "Monolithic sorbents for carbon dioxide removal," *Proc. 36th Int. Conf. on Environmental Systems (ICES)*, SAE International, Norfolk, VA, 2006-01–2193, 2006

[16]Wójtowicz, M. A., Rubenstein, E. P., Serio, M. A., and Cosgrove, J. E., "High-strength porous carbon and its multifunctional applications," US Pat. No. 8,615,812, 2013

[17]Wójtowicz, M. A., Markowitz, B. L., and Serio, M. A., "Microporosity development in carbons for gas-storage applications," *Proc. EUROCARBON '98: Science and Technology of Carbon*, AKK & GFEC, Strasbourg, France, 589–590, 1998

[18]Wójtowicz, M. A., Markowitz, B. L., Smith, W. W., and Serio, M. A., "Microporous carbon adsorbents for hydrogen storage," *Proc. Third International Conference on Materials Engineering for Resources (ICMR '98)*, Akita, Japan, 416–429, 1998

[19]Wójtowicz, M. A., Markowitz, B. L., Bassilakis, R., and Serio, M. A., "Hydrogen storage carbons derived from polyvinylidene chloride," presented at the 1999 Hydrocarbon Resources Gordon Research Conference, Ventura, CA, 1999

[20]Wójtowicz, M. A., Markowitz, B. L., Smith, W. W., and Serio, M. A., "Microporous carbon adsorbents for hydrogen storage," *Int. Journal of the Society of Materials Engineering for Resources*, **7**(2), 253–266, 1999

[21]Wójtowicz, M. A., Smith, W. W., Serio, M. A., Simons, G. A., and Fuller, W. D., "Microporous carbons for gas-storage applications," *Proc. Twenty-Third Biennial Conference on Carbon*, Pennsylvania State University, 342–343, 1997

[22]Simons, G. A., and Wójtowicz, M. A., "A model for microporosity development during char activation," *Proc. Twenty-Third Biennial Conference on Carbon*, Pennsylvania State University, 328–329, 1997

[23]Simons, G. A., and Wójtowicz, M. A., "Modeling the evolution of microporosity and surface area during char activation," *Proc. 9th Int. Conf. on Coal Science*, A. Ziegler, K. H. Van Heek, J. Klein, and W. Wanzl, eds., DGMK, Hamburg, Germany, 1783–1786, 1997

[24]Simons, G. A., and Wójtowicz, M. A., "Modeling the evolution of microporosity in a char-activation process involving alternating chemisorption-desorption cycles," *Proc. EUROCARBON '98: Science and Technology of Carbon*, AKK & GFEC, Strasbourg, France, 273–274, 1998

[25]Wójtowicz, M. A., Bassilakis, R., Leffler, M., Serio, M. A., and Fuller, W. D., "Adsorption of hydrogen on activated carbons derived from polyvinylidene chloride," *Proc. First World Conf. on Carbon EUROCARBON 2000*, Berlin, Germany, 407–408, 2000

[26]Wójtowicz, M. A., Rubenstein, E., and Serio, M. A., "Carbon-based sorbent for gas storage, and method for preparation thereof," US Pat. No. 8,231,712, 2012

[27]Walker, P. L., Jr., Austin, L. G., and Nandi, S. P., "Activated diffusion of gases in molecular-sieve materials," *Chemistry and Physics of Carbon*, P. L. Walker Jr., ed., Marcel Dekker, New York, 1966

[28]Cybulski, A., and Moulijn, J. A., "Monoliths in Heterogeneous Catalysis," *Catalysis Reviews*, **36**(2), 179–270, 1994

[29]Hawthorn, R. D., "Afterburner catalysis - effects of heat and mass transfer between gas and catalyst surface," *AIChE Symp. Ser.*, **70**(137), 428–438, 1974

[30]Shah, R. K., and London, A. L., *Laminar flow forced convection heat transfer and flow friction in straight and curved ducts - a summary of analytical solutions*, Dept. Mechn. Eng., Stanford University, Stanford, CA, n.d.